Biophysical response of living cells to boron nitride nanoparticles: Uptake mechanism and bio-mechanical characterization

Md. Alim Iftekhar Rasel[1], Tong Li[1], Trung Dung Nguyen[1], Sanjleena Singh[1], Yinghong Zhou[2], Yin Xiao[2] and YuanTong Gu[1]*

[1]School of Chemistry, Physics and Mechanical Engineering, Queensland University of Technology (QUT), Queensland, Australia, 4000
[2]Institute of Health and Biomedical Innovation, Queensland University of Technology (QUT), Queensland, Australia

*Corresponding author: yuantong.gu@qut.edu.au

Abstract

Boron nitride nanomaterials have attracted significant interest due to their superior chemical and physical properties. Despite these novel properties, investigation on the interaction between boron nitride nanoparticle (BN NP) and living systems has been limited. In this study, BN NP (100-250 nm) is assessed as a promising biomaterial for medical applications. The toxicity of BN NP is evaluated by assessing the cells behaviours both biologically (MTT assay, ROS detection etc.) and physically (Atomic Force Microscopy). The uptake mechanism of BN NP is studied by analysing the alternations in cellular morphology based on cell imaging techniques. The results demonstrate *in vitro* cytocompatibility of BN NP with immense potential for use as an effective nanoparticle for various biomedical applications.

Keywords: Boron nitride, Nanoparticles, Biomechanics, Cellular uptake mechanism, Cytotoxicity, Atomic Force Microscopy, Drug delivery vehicle.

Corresponding author: Prof. YuanTong Gu
Email: yuantong.gu@qut.edu.au
Tel: +61 07 3138 1009

Introduction

Nanoscale biomaterials (nanoparticles, nanotubes, nanowires etc.) have been subjected to intense study and evolution because of their excellent properties suitable for different biomedical applications (Gao and Xu 2009). In recent years, boron nitride (BN) nanomaterials (nanotubes/particles) have attracted significant interest due to their superior chemical and physical properties. However, in sharp contrast to many other nanomaterials (carbon nanotubes, gold nanoparticles etc), BN nanomaterials (nanoparticle/nanotubes) have been largely unexplored for advanced biomedical applications.

The combination of boron and nitrogen in order to form boron nitride does not occur naturally. They are carefully synthesized because of their attractive physical and chemical properties (Colombo 2010; Paine and Narula 1990). Boron nitride (BN) can be synthesized in different crystalline structures such as hexagonal, cubic, rhombohedral and turbostratic (Boulanger et al. 1995; Coles et al. 1969; Joni et al. 2011; Lian et al. 2010; Raidongia et al. 2010; Salles et al. 2009; Shi et al. 2008; Tang et al. 2008; Wood et al. 2005). Based on structural characteristics, BN demonstrates improved lubricating properties, resistance to chemical attack, resistance to oxidation, high thermal conductivity, excellent temperature resistance, low thermal expansion, better heat conductivity and excellent electrical insulation (Lian et al. 2010; Lin et al. 2009; Mosleh et al. 2009; Podobeda et al. 1976; Wu et al. 2001). Given all these unique properties, BN has a wide range of applications in different fields such as medical treatment, industrial tool manufacturing, electrical devices, photocatalysis and lubrication (Salles et al. 2012).

Studies have already been conducted to explore the superior characteristics of boron nitride nanotubes (BNNT). Chen et al. explored the use of BNNT as a drug delivery vehicle using single-stranded DNA as cargo (Chen et al. 2009). They found out that, FITC-DNA-BNNT was internalized successfully by the Chinese hamster ovary (CHO) cells. Ricotti et al. developed free standing polyacrilamide gels and used them on human fibroblast and murine myoblast with BNNT in order to control the skeletal muscle deformation at both gene and protein level (Ricotti et al. 2013). In a separate study, they successfully used glycol chitosan (GC) coated BNNT in an attempt to modulate F/G actin ratio and mechanical properties of human dermal fibroblasts (Ricotti et al. 2014).

Researchers have adopted different approaches to assess nanomaterials depending on their prospective applications. Recently, Ciofani et al. have conducted several studies in order to evaluate boron nitride nanotube (BNNT) (Ciofani et al. 2014; Ciofani et al. 2008). After conducting different assays and evaluating images of cells cultured with BNNT, they found BNNT to be safe and suitable for future biomedical use. Several other studies which also assessed the cytotoxicity of BNNT, support their claim (Chen et al. 2009; Del Turco et al. 2013). However, in a contrasting study, Horvath et al. found BNNT to be cytotoxic even in a very low concentrations in the investigated cell lines (Horvath et al. 2011). This highlights the influence of

particle characteristics and culture condition on the cytotoxicity of cells, further signifying the importance of proper evaluation of nanomaterials prior to practical use.

Nanoparticles are extremely popular in the field of biomedical engineering due to their unique structure, size and shape (De et al. 2008; Jin and Ye 2007; Steichen et al. 2013). Given these unique characteristics, BN NP can also be a crucial nanomaterial for advanced biomedical applications. However, the scope of BN NP as a biomaterial needs further strict evaluation. For instance, in the field of drug delivery; the effectiveness of nanoparticles can be hampered due to the low efficiency of delivery to the targeted cell population, inadequate cellular uptake and toxicity of nanoparticles. Therefore, researchers are continuously searching for safe and efficient nanoparticles (Hussain et al. 2009). For successful delivery of drugs, nanoparticles have to be efficiently taken in, be cytocompatible and facilitate normal functioning of living cells.

This study aims at evaluating BN NP as a potential biomaterial for future use. In order to investigate whether BN NP can be taken in by cells, osteoblast cells were cultured with BN NP in appropriate environment. Osteoblast cells play a crucial role in bone formation and are very popular in tissue engineering (Erisken et al. 2008; Zhang et al. 2008). Efforts have been made by researchers to better understand osteoblast-nanoparticle interaction for innovative tissue engineering applications in different studies (Liang et al. 2011; Pauksch et al. 2014; Shi et al. 2009). In order to confirm the uptake of BN NP, osteoblast cells were sectioned in very fine slices and evaluated visually using transmission electron microscopy (TEM). The penetration mechanism and particle distribution in cells were analysed. The cytotoxicity of BN NP was evaluated using the traditional MTT as well as ROS detection assay. Later the mechanical properties of cells were characterized using spectroscopy techniques to understand the changes of mechanical performances due to BN NP uptake.

Materials and methods

Preparing the nanoparticles

BN NP's (Trade Name: TECO20051158 Boron nitride powder, purity 90%) were sourced from Momentive Performance Materials Inc. (Ohio, USA). The particles were in white powder state with a melting point of 3000°F. The bulk density of the particles ranged from 2.1-2.2 g/cc. The nanoparticles were prepared by adding varying amount of UHQ water to dilute them at different concentrations. The solution was then ultrasonicated for 4h at ambient temperature (Misonix Sonicator, 3000). After that, solution was sterilized by autoclaving at 121° C for 20 mins before future cell works. Prior to all the cell works, an ethical clearance was obtained from University Human Research Ethics Committee (QUT approval number: 1400001024).

Cell culture

In this study, osteoblast cells were used as samples. Cells were seeded into six well plates and cultured using Dulbecco's Modified Eagle's Medium (low glucose) (GIBCO, Invitrogen Corporation, Melbourne, Australia) supplemented with 10% fetal bovine serum (FBS) (HyClone, Logon, UT) and 1% penicillin and streptomycin (P/S) (GIBCO, Invitrogen Corporation, Melbourne, Australia). The cells were placed in a secure environment depicting the human body conditions (37°C in a humidified atmosphere with 6% CO_2). After cells were confluent, they were detached using 0.5% Trypsin (Sigma-Aldrich) and distributed into other flasks and dishes. Cells were further processed depending on the experiments (AFM, TEM, Confocal etc.) performed.

X-ray spectroscopy

The XRD patterns were recorded on a Philips PANalytical X'pert pro diffract meter. A fixed power source (40 mA) and Cu Ka radiation (40 kV) were used. The data were collected between a 2θ (between 3.5 and 75) at a scanning rate of 2.5 degree min^{-1}.

Transmission Electron Microscopy

Samples were properly processed in a step by step manner (buffer wash, post fixation, dehydration, resin implantation) before being imaged using transmission electron microscopy (TEM). The cultured cells were fixed using 3% Glutaraldehyde (10min) and rinsed twice using 0.1M Cacodylate buffer (20min). Then, they were treated with 1% Osmium Tetroxide for an hour. They were rinsed again with UHQ water thrice (10 min each) before being treated with 1% Uranyl Acetate for an hour. Cells were then dehydrated by multiple exchanges of ethanol, using progressively higher ethanol concentrations starting from 50% and up to 100%. This was followed by resin (LX112) implantation in the culture dish. The concentration of the resin was

varied from a low to high resin ethanol ratio (1:2, 1:1, 2:1). Finally the cells were treated with 100% percent resin (1h) before being put in the oven at 70°C (24h).

The processed samples were then sectioned in 80 nm thickness using the Leica UC7 Ultramicrotome. The sectioned samples were placed in a 400 mesh carbon grids and imaged using the JOEL TEM 1400.

Atomic Force Microscopy

The osteoblast cells with and without BN NP were cultured and prepared properly before being tested on AFM. The cells with particles were cultured for 24h with BN NP at a concentration of 30 µg/ml. Cells were then detached from the substrate using 0.5% of Trypsin (Sigma-Aldrich) and seeded in a petri dish coated with poly-D-lysone (PDL, Sigma-Aldrich). Afterwards, they were allowed to sit in the incubator for 1-1.5 hours to form a strong attachment while keeping the cell morphology round. The testing was conducted at room temperature.

The Atomic Force Microscope (AFM) used in current study is a Nanosurf FlexAFM (Nanosurf AG, Switzerland), which is mounted with a Leica DM IRB. The SHOCONG-SiO_2-A-5 (AppNano) colloidal probe cantilever was used for the indentation (Fig- 1). The probe is of 5 µm diameter and has a spring constant of 0.224-0.3114 N/m which was determined by the thermal noise function.

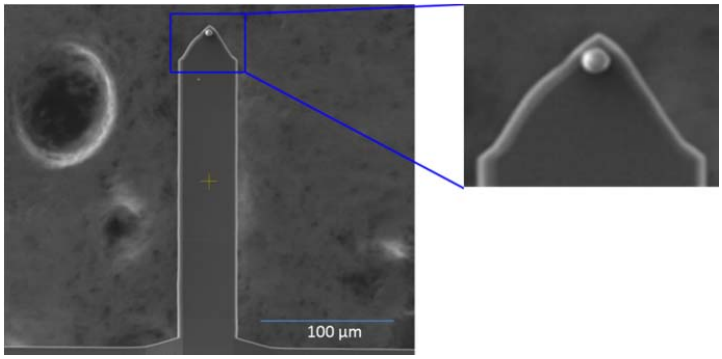

Fig 1 SEM image of colloidal probe cantilever SHOCONG-SiO2-A-5 (AppNano) used in this study (The inset shows the real diameter of the bead).

To investigate the mechanical properties of human osteoblast cells, Young's modulus of each cell was obtained from the force indentation curves using the modified Hertzian model proposed

by Dimitriadis et al (Dimitriadis et al. 2002). As colloidal probe cantilevers were used for this study, the relationship between the force (F) and indentation (δ) can be expressed as,

$$F = \frac{4E}{3(1-\nu^2)} R^{\frac{1}{2}} \delta^{\frac{3}{2}} \left[1 - \frac{2\alpha_0}{\pi}\chi + \frac{4\alpha_0}{\pi^2}\chi^2 - \frac{8}{\pi^3}\left({\alpha_0}^3 + \frac{4\pi^2}{15}\beta_0 \right)\chi^3 + \frac{16\alpha_0}{\pi^4}\left({\alpha_0}^3 + \frac{3\pi^2}{5}\beta_0 \right)\chi^4 \right] \quad (1)$$

Here, $\chi = \sqrt{\frac{R\delta}{h}}$, α_0 and β_0 are the functions of Poisson's ratio ν, R is the radius of the rigid indenter and E is Young's modulus. For simplicity, Poisson's ratio of the osteoblast cells was assumed to be 0.5 (Zhou et al. 2005).

As the cells have strong attachment with the substrate, α_0 and β_0 can be expressed as,

$$\alpha_0 = -\frac{1.2876 - 1.4678\nu + 1.3442\nu^2}{1-\nu} \quad (2)$$

$$\beta_0 = \frac{0.6387 - 1.0277\nu + 1.5164\nu^2}{1-\nu} \quad (3)$$

The force-indentation curves obtained from the indentation test were further processed using the Scanning Probe Image Processor (SPIP 6.3.3). In order to get Young's modulus from the force-indentation curve, a Matlab (The MathWorks, Inc.) program was developed based on the automatic force curve analysis algorithm proposed by Lin et al (Lin et al. 2007).

Confocal Imaging

The osteoblasts were cultured with BN NP with varied culture times depending on the experimental requirements. Once the specified culture time was achieved, the cells were gently washed with PBS (Sigma-Aldrich). The cells were then fixed with 4% Paraformaldehyde (Sigma-Aldrich) for 20 minutes. The samples were repeatedly washed in PBS for several minutes in order to remove any unwanted agents. Cells were then permeabilized with 0.1% Triton X100 (Sigma-Aldrich).

After a few more washes with PBS, the samples were then incubated with 1:100 of DAPI and Alexa Fluor 568 Phalloidin (GIBCO, Invitrogen Corporation, Melbourne, Australia) for 10-15 minutes in order to stain the nuclei and actin filament networks respectively. The samples were then washed one more time and were taken to a confocal microscope (Nikon A1R confocal, Japan) for the purpose of imaging. The 40X oil immersion objective lens was used.

MTT Assay

The cellular metabolic activity of the osteoblasts cells in the various BN NP solutions was assessed using the 3-(4,5-dimethylthiazol-2-yl)-2,5-diphenyltetrazolium bromide (MTT) assay. In brief, cells were cultured in 96-well plates at an initial density of 5×10^3 cells in 200 mL of medium containing various concentrations of BN. On day 1, 3 and 5, 20 mL of 5 mg/mL of MTT solution (Sigma–Aldrich, Australia) was added to each well and incubated at 37 °C for 4 h to form the formazan crystals. Then the media were replaced by 100 mL of dimethyl sulfoxide (DMSO; Sigma–Aldrich, Australia) to dissolve the formazan. The absorbance was measured at λ= 495 nm using a SpectraMax Microplate Reader (Molecular Devices, Inc., USA).

Cellular ROS Detection

Cellular ROS detection assay was performed according to the protocol for the DCFDA Cellular ROS Detection Assay Kit (Abcam, Cambridge, United Kingdom). Osteoblasts with $2x10^4$ cells/ml were seeded on 96-well plate and left overnight to attach. Next day, growth medium was removed and replaced with serum free DMEM with BN NP (with varying concentration) for 24 hours. On the day of experiment, cells were incubated with DCFDA reagent for 45 minute at 37°C in the dark. The fluorescence was read using fluorescence plate reader to perform an endpoint read at 485 nm excitation wavelength and 535 nm emission wavelength.

Results and discussions

Nanoparticle Characterization

Boron nitride consists of equal number of boron and nitrogen atoms. It is isoelectronic to similar structured carbon lattice and therefore exists in different crystalline forms. Several tests such as Energy-dispersive X-ray spectroscopy (EDS) and X-ray Diffraction (XRD) were carried out to confirm the material as boron nitride. Moreover, the size and the shape of the particles were unveiled using transmission electron microscopy (TEM) images from representative samples.

The EDS demonstrates the material consists of boron (49%) and nitrogen (49%) confirming the material as boron nitride (Fig-2a). The XRD result indicates they are well crystallized (Fig-2b). From the TEM images, the particles are found to be of varying shape with their size ranging from 100-250 nm (Fig- 2a).

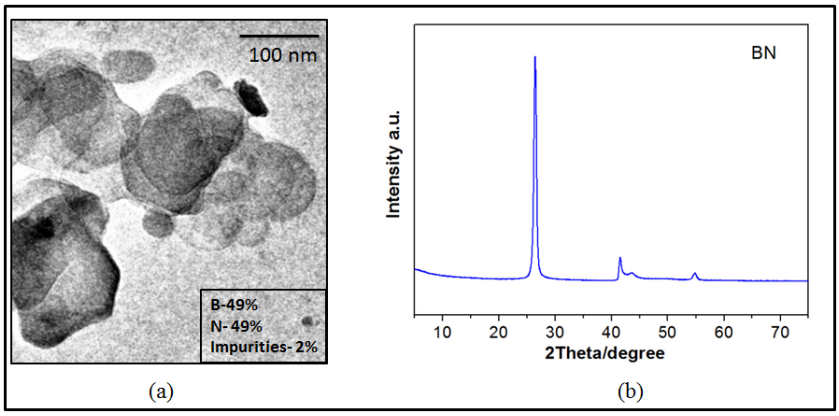

Fig 2 (a) EDS results showing 49% Boron and 49% Nitrogen content. (b) XRD results indicating the crystallinity of the material.

Toxicity of BN NP

In this study, we have adopted MTT assay (3-(4,5-dimethylthiazol-2-yl)-2,5-diphenyltetrazolium bromide) and reactive oxygen species (ROS) production to assess the cytocompatibility of BN NP. Although few studies have previously been conducted assessing the biocompatibility of boron nitride nanotubes and nanorods, this is the first study investigating the biocompatibility of boron nitride nanoparticles (BN NP).

For the MTT assay, osteoblast cells were cultured with BN NPs for three different time periods (day 1, 3, 5) with varying concentrations (0, 20, 30, 50, 200 µg/ml). The results are shown in Fig 3.

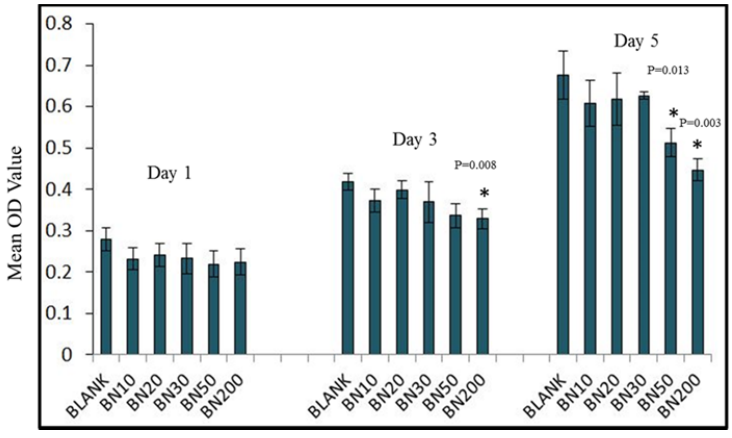

Fig 3 The overall metabolic activity of osteoblast cells indicated by MTT, with increasing concentration of BN NP. The concentration varies from none (blank) to 200 µg/ml. BN10, BN20, B30, BN50 and BN200 indicate the concentrations 10 µg/ml, 20 µg/ml, 30 µg/ml, 50 µg/ml and 200 µg/ml, respectively. (* indicate statistically significant change in the value.)

The MTT results show that the overall metabolic activity of all cells increased with the incubation time for all groups. This demonstrates normal growth of cells in the medium. However, there is essentially little to no difference (statistically insignificant) between the metabolism of normal cells and the cells with BN NPs in different incubation time, except for high BN NP concentration (50 µg/ml, 200µg/ml).

In order to better evaluate the cellular response to the nanoparticle uptake, the ROS production test was also carried out. Osteoblast cells were cultured in 96 well plates with varying concentration of BN NP (0, 10, 20, 30,40, 50 µg/ml). The production of oxygen was quantified as florescent intensity. The results are shown in Fig 4. A significant production of ROS can be observed for all nanoparticle concentrations**.** The increasing nanoparticle concentration does not show any real effect in terms of ROS production and cytotoxicity. Cells are found to adapt quite well to the nanoparticle. Overall, The MTT assay and the ROS production test clearly indicates that BN NP is cytocompatible (in vitro) and should be safe to be used for advanced biomedical engineering applications.

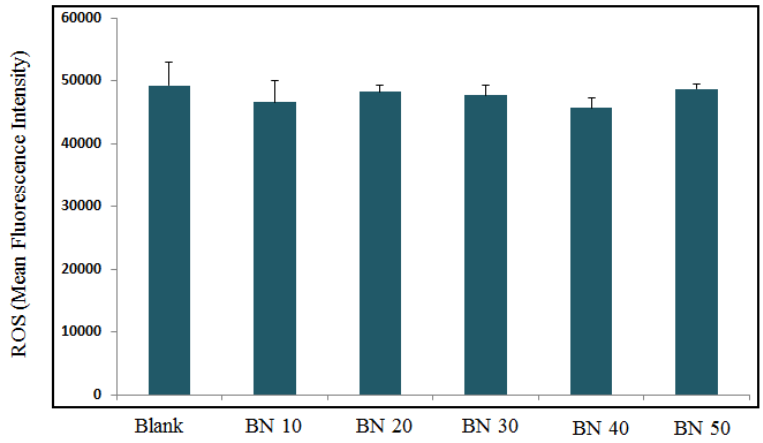

Fig 4 The quantification of ROS levels in osteoblast cells exposed in different concentration of BN NP. The concentration varies from none (blank) to 50 µg/ml. BN10, BN20, BN30, BN 40 and BN50 indicate the concentrations 10 µg/ml, 20 µg/ml, 30 µg/ml, 40 µg/ml and 50 µg/ml respectively.

Cellular Uptake Mechanism

It has already been established through the MTT assay and ROS production test that BN NPs do not affect the cell viability to a great extent. Now, it is vital to investigate the mechanisms dictating the cell and nanoparticle interaction (uptake process, drug coating suitability etc.) depending on specific biomedical applications (drug delivery vehicle, tissue engineering, implants etc.). In this study, our main focus was the physical aspects of the interaction between cell and nanoparticle.

To identify the uptake of BN NP, osteoblast cells were cultured with BN NPs for different time periods. There are several available experimental techniques that could have been adopted for this test. The most commonly used technique for characterization of nanoparticle along with cells is confocal microscopy. However, due to the limited resolution of this technique, it is hard to conclude whether the nanoparticles are taken in by the cell or just bound to the cell surface. Transmission electron microscopy (TEM), on the other hand facilitates higher quality imaging where the material can be cut and observed in nanoscale slides. Hence, TEM characterization was adopted to identify the actual position of BN NP within the cell. The osteoblast cells were sectioned in very thin slides using ultramicrotome (80 nm, details can be found in the section of Material and Methods) before being imaged in TEM.

Fig -5 shows a sectioned human osteoblast cell after being cultured by BN NPs for 24 hours. The plasma membrane and nucleus can be clearly identified. BN NP can be clearly observed randomly locating throughout the cytoplasm. This proves that osteoblast cells happily take in BN NP. This is crucial for potential use of BN NP for future biomedical applications like tissue engineering, gene delivery, nanovector, nano imaging and so on.

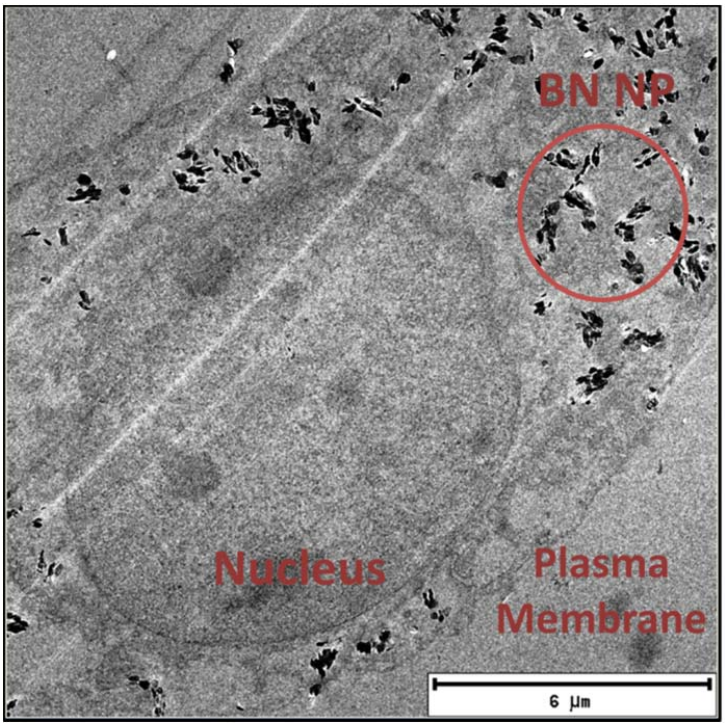

Fig 5 A TEM image of a sectioned osteoblast cell after being cultured by BN NP for 24 hours.

The interaction mechanisms between living systems and materials are attracting more and more attention due to their potential to provide insightful feedback for sophisticated biomaterial designs (Iversen et al. 2011; Lesniak et al. 2012; Nativo et al. 2008). Therefore it is necessary to

study the physical mechanisms of cellular uptake process of BN NPs. After extensive analysis of TEM images of osteoblast cells (cultured with BN NPs), it was found that the cellular uptake process of BN NPs can be generally divided into three stages: the adhesion to cell membrane, particle invagination and particle internalization. Detailed illustration of each stage is provided in Figs 6-8 respectively.

When the nanoparticles are suspended in the cell medium, a good number of particles end up on the cell surface due to physical sedimentation of particles and adhesive characteristics of the plasma membrane. The cells come into contact with the remaining particles when they are spreading naturally. The uptake process begins with an initial contact adhesion between the cell membrane and nanoparticle. The same phenomenon can be observed for all cells irrespective of culture time. This is the first step of the particle uptake process and can be clearly observed from Fig -6. It is also consistent with previous observations (Lesniak et al. 2013).

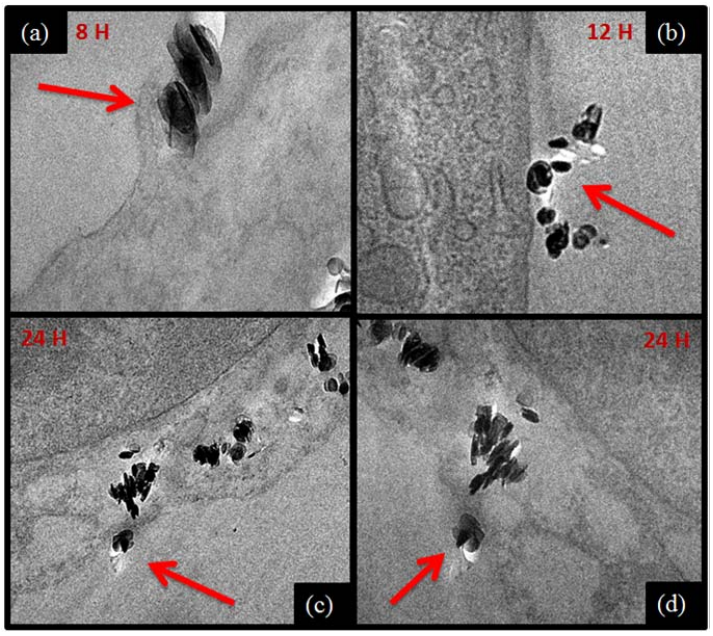

Fig 6 The initial contact between the cell and BN NP at different culture time.

Once the particle adheres to the cell membrane, the cell membrane folds backwards to form a cavity and tries to cover the particle from all directions (Fig -7). This is the second step of the uptake process and we will call it invagination. The invagination of the cell membrane indicates the uptake process to be endocytosis (Colognato et al. 2012).

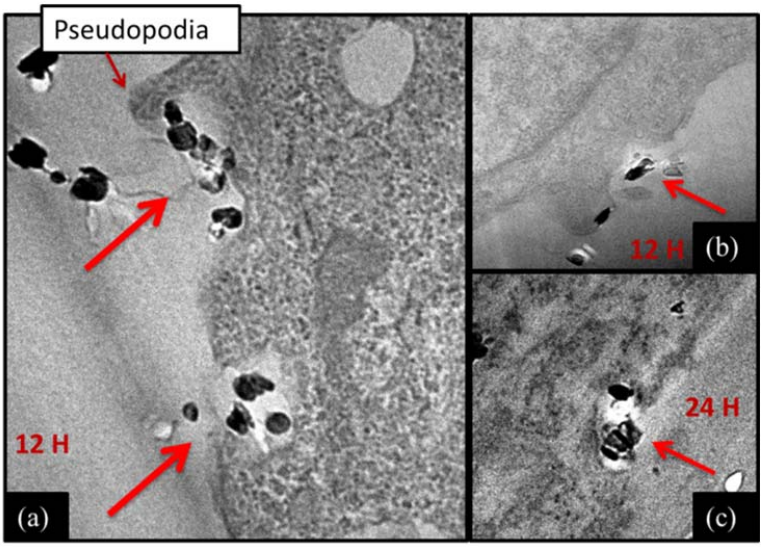

Fig 7 The invagination of cell membrane. TEM image of osteoblast cell cultured with BN NP for different culture time

Once the particles are covered by the cell membrane, they are transported from the membrane to the cytoplasm. We call this step particle internalization. The particles are separated from the other cytoplasmic components by creating a circular cavity (Fig -8). As particles can internalize from any direction, they are distributed throughout the whole cytoplasm.

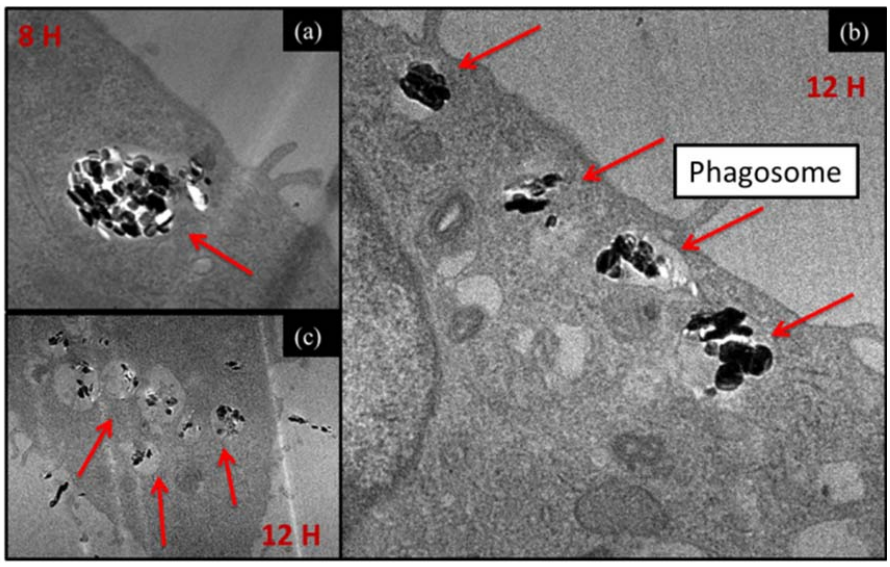

Fig 8 The internalization of BN NP in the cell cytoplasm. TEM image of osteoblast cell cultured with BN NP for different culture time

After careful study of the TEM images, the uptake process can be confirmed as typical endocytosis. Now, endocytosis can be of different types; phagocytosis (cell eating), pinocytosis (cell drinking), receptor mediated endocytosis and so on. Ideally, for nano-sized materials, cells tend to adopt micropinocytosis. However, careful study indicates that, the uptake process of BN NP by osteoblast cells is in fact phagocytosis, as all the steps of phagocytosis can be clearly identified. Once the BN NP's stick to the plasma membrane, the cell recognizes the material and makes a conscious effort to protrude towards the nanoparticles (Fig- 7). The membrane projection generated by the cell to engulf the nanoparticle from all directions is normally called pseudopodia. Once the BN NP's are engulfed, large vesicles are formed to transport the nanoparticles from the membrane to the cytoplasm (Fig- 8). These large vesicles are normally known as phagosomes. The phagocytosis of BN NP instead of micropinocytosis is understandable because of the relatively larger size of BN NP (100-250 nm). Similar phenomenon was also observed in previous studies (Gupta et al. 2004).

In order to further establish that the particle uptake process of BN NP by osteoblast cells is indeed endocytosis, we adopted a unique approach. Two sets of osteoblast cells were separately cultured in a 6 well plate for 24 hours, referred to as set A and set B. After the cells were confluent, set A was treated with Cytochalasin D at a concentration of 5 μg/ml for 30 min. Cytochalasin D is known to inhibit endocytosis (specially phagocytosis, micropinocytosis) and is widely used for in vitro research (Dutta and Donaldson 2012; Herre et al. 2004; Stevenson and Begg 1994). Both set A and B were then cultured with BN NP at a concentration of 20 μg/ml. After 24h, the solution of each culture medium (set A and B) was collected and the concentrations of BN NP in each solution quantified using a spectrophotometer (Cary 60 UV-Vis spectrometer). Spectrophotometric determination is a unique method to quantify concentration of nanoparticle in a solution (Maye et al. 2003; Unciti-Broceta et al. 2015). The system was properly calibrated by scanning a series of standardized solutions (BN concentration from 0-50 μg/ml) before the concentration of set A and B were quantified.

As Cytochalasin D is bound to inhibit endocytosis and if endocytosis is indeed the principle uptake mechanism of BN NP uptake, set A is less likely to uptake any nanoparticle whereas set B is expected to uptake BN NP normally.

Fig- 9 demonstrates the concentration of BN NP (expressed in percentage in relation to the initial concentration; 20 μg/ml) in the culture medium after 24h. The concentration of BN NP in set A is found to be around 82.5% whereas in set B it is 19.5%. Under normal conditions cells seems to uptake a lot of particles (set B). However, if the endocytic pathways are blocked (set A) cells barely take in any particles at all. This result clearly establishes the uptake mechanism of BN NP by osteoblast cells as endocytosis.

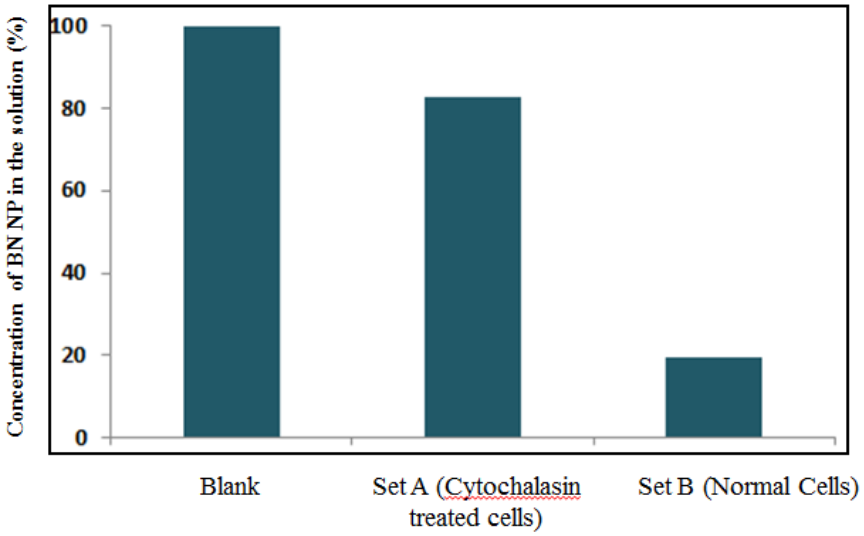

Fig 9 Concentration of BN NP in the solutions (Both set A and B) expressed in percentages. Set A represents cells treated with Cytochalasin D before being cultured with BN NP at a concentration of 20 µg/ml for 24 hours. Set Set B represents cells cultured with BN NP at a concentration of 20 µg/ml for 24 hours.

Apart from the mechanism, another vital aspect of the uptake process is observed. In one particular time frame, BN NPs were observed to be in different stages of the uptake mechanism. Some particles were observed to stick to the plasma membrane after 24 h (Fig- 6c&d) whereas others were observed to be internalized after just 8 h (Fig- 8a). Therefore, it can be concluded that, the cellular uptake of BN NP is not a linear process. It is independent of the culture time.

Localization of BN NP

The localization of nanoparticles in the cell is particularly important for specific biomedical applications. Osteoblast cells were cultured with BN NP for 24 hours and imaged with both TEM and confocal to obtain a visual demonstration of nanoparticles positions in the cytoplasm. Fig - 10 represents confocal image of osteoblast cells with and without nanoparticles. Cells are observed to be spreading in different directions with the actin filament (red) and the nucleus (blue) clearly visible. The BN NP's (green) are observed to be distributed throughout the F-actin network around the nucleus. A significant number of particles are observed to be taken in by the osteoblast cells.

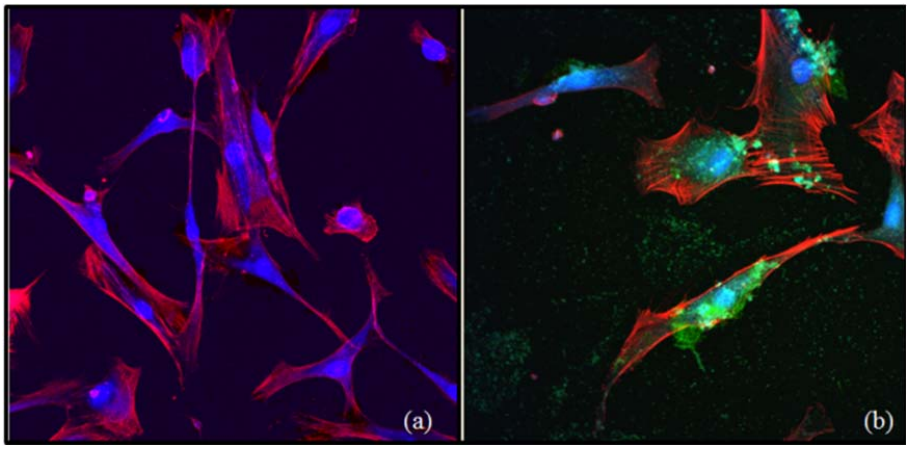

Fig 10 Confocal Image of osteoblast cells without (a) and with (b) BN NP

Fig- 11 demonstrates a typical TEM image of osteoblast cells cultured with BN NP's. The image is enlarged in order to better observe the distribution of nanoparticles in the cell cytoplasm (Fig-11 b&c). It can be observed that nanoparticles are not uniformly distributed; rather they are clustered together in different parts of the cells indicating signs of aggregation. However, as observed in the confocal images, a significant number of BN NPs are observed to be distributed throughout the cytoplasm which is an encouraging sign.

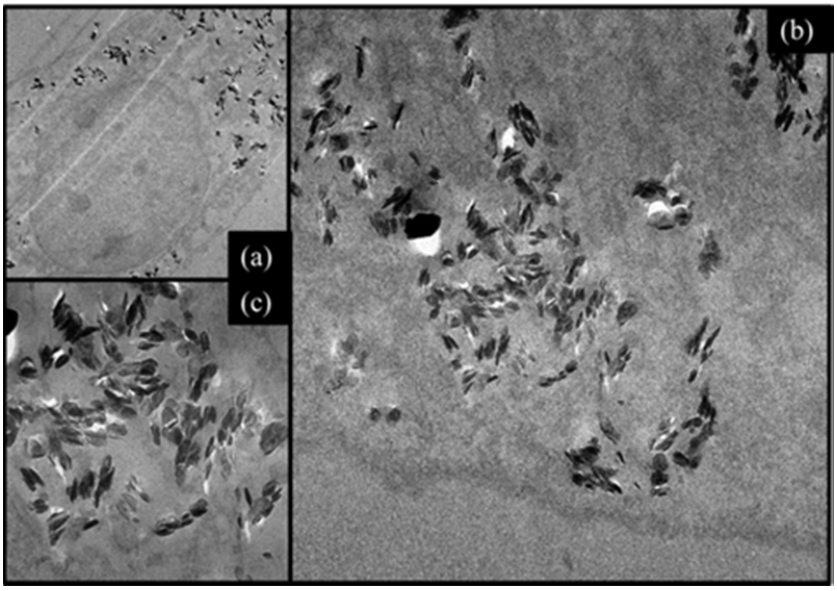

Fig 11 TEM Image of osteoblast cells surface with BN NP.

Investigating the mechanical response

It should be noted that although the BN NP does not have adverse effect on the viability/metabolism of the cells, it is still a concern whether BN NP will change the biochemical and biomechanical properties of the cells. As physical entities, cells possess structural integrity that enables them to withstand the mechanical stimuli it is subjected to. For proper functioning of the human body, cell structure and mechanical properties have to be retained. Any deviation may cause breakdown of physiological functions and lead to diseases. For example, the deterioration of the mechanical properties of chondrocyte cells is believed to be one of the main factors in the development and progression of osteoarthritis (Trickey et al. 2000). In this study, we aimed to assess the physical response of cells to BN NP uptake and thereby test the physical wellbeing of cells. This is a new and innovative approach of evaluating the cytocompatibility of nanomaterials from a physical point of view.

We adopted Atomic Force Microscopy (AFM) to conduct this bio-mechanical characterization. In AFM, a flexible cantilever fitted with a tip of microscopic dimension is used to indent the material/sample and Young's modulus is measured from the generated force-indentation (F-δ) curve (Darling et al. 2006; Faria et al. 2008; Ladjal et al. 2009). Recently Trung et al. have successfully developed a technique to test the mechanical stiffness of different cells using AFM (Nguyen and Gu 2014a; Nguyen and Gu 2014b). The aim was to quantify the stiffness of both normal cells and cells cultured with BN NP to assess them in relation to biosafety.

An approach similar to Trung et al. was adopted to quantify the stiffness of cells. Both normal cells (n=35) and cells cultured with BN NP (n=37) were processed before being tested in AFM (details in Methods and materials). Fig- 12 shows Young's modulus of both variations and it can be observed that there is little difference between them (statistically insignificant). Despite taking in a significant amount of nanoparticles, cells are still as stiff as they were before. This is significant, because it indicates that even though nanoparticles are spread in the cell cytoplasm, structural stability is not compromised. Cells are still functioning normally as cells without BN NPs.

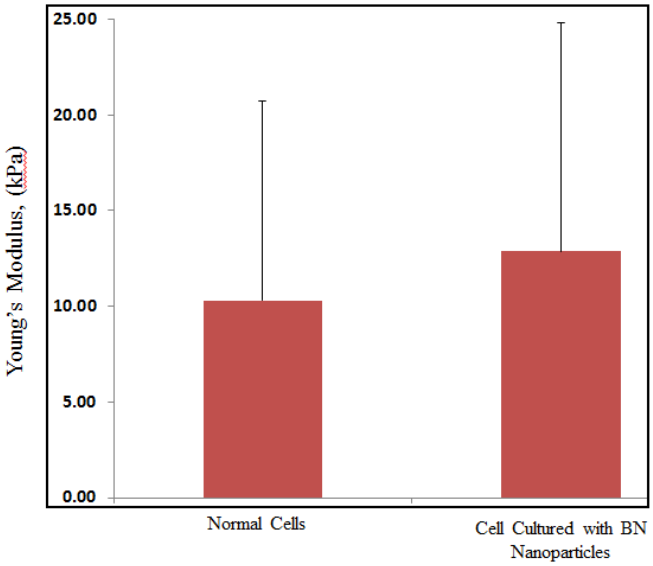

Fig 12 Comparing Young's Modulus between normal cells and cells cultured with BN NP at a concentration of 30 µg/ml.

Conclusion

This study confirmed BN NP as a potential candidate for advanced biomedical engineering applications. The MTT assays and ROS production study showed BN NP (100-250 nm) does not have adverse effects on the viability/ metabolism of osteoblast cells. The transmission electron microscopy (TEM) images showed that BN NP's are successfully internalized by the cells. The interaction of osteoblast cells and BN NP was extensively studied through analysing images taken by TEM and confocal microscopy. The complete uptake process of BN NP was uncovered which is distinctly divided in three separate stages: adhesion to cell membrane, invagination and internalization. The uptake mechanism was identified as phagocytosis and different stages of phagocytosis were also identified. The localization of BN NP inside the cell was also studied and analysed. A significant amount of nanoparticles were observed to be taken in by osteoblast cells. The effect of nanoparticle uptake on the mechanical stiffness of cells was also studied. It was observed that despite significant BN NP uptake, there was no change in the cell stiffness. This signifies cells still maintained their structural integrity.

Collectively these experimental works enable us to develop a better understanding of the interaction between BN NP and osteoblast cells before being used in an *in vivo* situation. Initial results confirm BN NP to be a potential candidate for sophisticated biomedical engineering applications (drug delivery, gene delivery, cell therapy etc.) and calls for more research efforts in this field.

Acknowledgement

This research was funded by ARC Future Fellowship project (No. FT100100172), ARC Discovery Project: DP150100828 and QUT Postgraduate Research Award (QUTPRA). This work was performed in part at the central analytical and research facility (CARF) and Institute of Health and Biomedical Innovation (IHBI, QUT). The authors gratefully acknowledge Mr. Arixin Bo for his assistance in X-ray Diffraction of BN NP. The authors also acknowledge Miss Saba Farnaghi for her help with ROS production study.

Reference

Boulanger L, Andriot B, Cauchetier M, Willaime F (1995) Concentric shelled and plate-like graphitic boron nitride nanoparticles produced by CO2 laser pyrolysis Chemical Physics Letters 234:227-232 doi:http://dx.doi.org/10.1016/0009-2614(95)00008-R

Chen X, Wu P, Rousseas M, Okawa D, Gartner Z, Zettl A, Bertozzi CR (2009) Boron nitride nanotubes are noncytotoxic and can be functionalized for interaction with proteins and cells Journal of the American Chemical Society 131:890-891

Ciofani G et al. (2014) Cytocompatibility evaluation of gum Arabic-coated ultra-pure boron nitride nanotubes on human cells Nanomedicine 9:773-788

Ciofani G, Raffa V, Menciassi A, Cuschieri A (2008) Cytocompatibility, interactions, and uptake of polyethyleneimine-coated boron nitride nanotubes by living cells: Confirmation of their potential for biomedical applications Biotechnology and bioengineering 101:850-858

Coles N, Glasson D, Jayaweera S (1969) Formation and reactivity of nitrides. III. Boron, aluminium and silicon nitrides Journal of Applied Chemistry 19:178-181

Colognato R, Park M, Wick P, De Jong WH (2012) Interactions with the Human Body Adverse Effects of Engineered Nanomaterials: Exposure, Toxicology and Impact on Human Health

Colombo P (2010) Polymer derived ceramics: from nano-structure to applications. DEStech Publications, Inc,

Darling E, Zauscher S, Guilak F (2006) Viscoelastic properties of zonal articular chondrocytes measured by atomic force microscopy Osteoarthritis and Cartilage 14:571-579

De M, Ghosh PS, Rotello VM (2008) Applications of nanoparticles in biology Advanced Materials 20:4225-4241

Del Turco S et al. (2013) Cytocompatibility evaluation of glycol-chitosan coated boron nitride nanotubes in human endothelial cells Colloids and Surfaces B: Biointerfaces 111:142-149

Dimitriadis EK, Horkay F, Maresca J, Kachar B, Chadwick RS (2002) Determination of elastic moduli of thin layers of soft material using the atomic force microscope Biophysical journal 82:2798-2810

Dutta D, Donaldson JG (2012) Search for inhibitors of endocytosis Cellular Logistics 2:203-208 doi:10.4161/cl.23967

Erisken C, Kalyon DM, Wang H (2008) Functionally graded electrospun polycaprolactone and β-tricalcium phosphate nanocomposites for tissue engineering applications Biomaterials 29:4065-4073 doi:http://dx.doi.org/10.1016/j.biomaterials.2008.06.022

Faria EC, Ma N, Gazi E, Gardner P, Brown M, Clarke NW, Snook RD (2008) Measurement of elastic properties of prostate cancer cells using AFM Analyst 133:1498-1500

Gao J, Xu B (2009) Applications of nanomaterials inside cells Nano Today 4:37-51 doi:http://dx.doi.org/10.1016/j.nantod.2008.10.009

Gupta AK, Gupta M, Yarwood SJ, Curtis AS (2004) Effect of cellular uptake of gelatin nanoparticles on adhesion, morphology and cytoskeleton organisation of human fibroblasts Journal of Controlled Release 95:197-207

Herre J et al. (2004) Dectin-1 uses novel mechanisms for yeast phagocytosis in macrophages Blood 104:4038-4045 doi:10.1182/blood-2004-03-1140

Horvath L et al. (2011) In vitro investigation of the cellular toxicity of boron nitride nanotubes ACS nano 5:3800-3810

Hussain SM et al. (2009) Toxicity evaluation for safe use of nanomaterials: recent achievements and technical challenges Advanced Materials 21:1549-1559

Iversen T-G, Skotland T, Sandvig K (2011) Endocytosis and intracellular transport of nanoparticles: present knowledge and need for future studies Nano Today 6:176-185

Jin S, Ye K (2007) Nanoparticle-Mediated Drug Delivery and Gene Therapy Biotechnology Progress 23:32-41 doi:10.1021/bp060348j

Joni IM, Balgis R, Ogi T, Iwaki T, Okuyama K (2011) Surface functionalization for dispersing and stabilizing hexagonal boron nitride nanoparticle by bead milling Colloids and Surfaces A: Physicochemical and Engineering Aspects 388:49-58 doi:http://dx.doi.org/10.1016/j.colsurfa.2011.08.007

Ladjal H, Hanus JL, Pillarisetti A, Keefer C, Ferreira A, Desai JP Atomic force microscopy-based single-cell indentation: Experimentation and finite element simulation. In: Intelligent Robots and Systems, 2009. IROS 2009. IEEE/RSJ International Conference on, 10-15 Oct. 2009 2009. pp 1326-1332. doi:10.1109/IROS.2009.5354351

Lesniak A, Fenaroli F, Monopoli MP, Åberg C, Dawson KA, Salvati A (2012) Effects of the presence or absence of a protein corona on silica nanoparticle uptake and impact on cells ACS nano 6:5845-5857

Lesniak A, Salvati A, Santos-Martinez MJ, Radomski MW, Dawson KA, Åberg C (2013) Nanoparticle Adhesion to the Cell Membrane and Its Effect on Nanoparticle Uptake Efficiency Journal of the American Chemical Society 135:1438-1444 doi:10.1021/ja309812z

Lian G, Zhang X, Zhu L, Tan M, Cui D, Wang Q (2010) A facile solid state reaction route towards nearly monodisperse hexagonal boron nitride nanoparticles Journal of Materials Chemistry 20:3736-3742 doi:10.1039/B920881J

Liang C, Joseph MM, James CML, Hao L (2011) The role of surface charge on the uptake and biocompatibility of hydroxyapatite nanoparticles with osteoblast cells Nanotechnology 22:105708

Lin DC, Dimitriadis EK, Horkay F (2007) Robust strategies for automated AFM force curve analysis—I. Non-adhesive indentation of soft, inhomogeneous materials Journal of biomechanical engineering 129:430-440

Lin L, Li Z, Zheng Y, Wei K (2009) Synthesis and application in the CO oxidation conversion reaction of hexagonal boron nitride with high surface area Journal of the American Ceramic Society 92:1347-1349

Maye MM, Han L, Kariuki NN, Ly NK, Chan W-B, Luo J, Zhong C-J (2003) Gold and alloy nanoparticles in solution and thin film assembly: spectrophotometric determination of molar absorptivity Analytica chimica acta 496:17-27

Mosleh M, Atnafu ND, Belk JH, Nobles OM (2009) Modification of sheet metal forming fluids with dispersed nanoparticles for improved lubrication Wear 267:1220-1225 doi:http://dx.doi.org/10.1016/j.wear.2008.12.074

Nativo P, Prior IA, Brust M (2008) Uptake and Intracellular Fate of Surface-Modified Gold Nanoparticles ACS Nano 2:1639-1644 doi:10.1021/nn800330a

Nguyen TD, Gu Y (2014a) Determination of Strain-Rate-Dependent Mechanical Behavior of Living and Fixed Osteocytes and Chondrocytes Using Atomic Force Microscopy and Inverse Finite Element Analysis Journal of biomechanical engineering 136:101004

Nguyen TD, Gu Y (2014b) Exploration of mechanisms underlying the strain-rate-dependent mechanical property of single chondrocytes Applied Physics Letters 104:183701 doi:doi:http://dx.doi.org/10.1063/1.4876056

Paine RT, Narula CK (1990) Synthetic routes to boron nitride Chemical Reviews 90:73-91

Pauksch L, Hartmann S, Rohnke M, Szalay G, Alt V, Schnettler R, Lips KS (2014) Biocompatibility of silver nanoparticles and silver ions in primary human mesenchymal stem cells and osteoblasts Acta Biomaterialia 10:439-449 doi:http://dx.doi.org/10.1016/j.actbio.2013.09.037

Podobeda L, Tsapuk A, Buravov A (1976) Oxidation of boron nitride under nonisothermal conditions Soviet Powder Metallurgy and Metal Ceramics 15:696-698

Raidongia K, Gomathi A, Rao CNR (2010) Synthesis and Characterization of Nanoparticles, Nanotubes, Nanopans, and Graphene-like Structures of Boron Nitride Israel Journal of Chemistry 50:399-404 doi:10.1002/ijch.201000047

Ricotti L et al. (2014) Boron nitride nanotube-mediated stimulation modulates F/G-actin ratio and mechanical properties of human dermal fibroblasts Journal of nanoparticle research 16:1-14

Ricotti L et al. (2013) Boron nitride nanotube-mediated stimulation of cell co-culture on micro-engineered hydrogels PloS one 8:e71707

Salles V, Bernard S, Chiriac R, Miele P (2012) Structural and thermal properties of boron nitride nanoparticles Journal of the European Ceramic Society 32:1867-1871

Salles V, Bernard S, Li J, Brioude A, Chehaidi S, Foucaud S, Miele P (2009) Design of highly dense boron nitride by the combination of spray-pyrolysis of borazine and additive-free sintering of derived ultrafine powders Chemistry of Materials 21:2920-2929

Shi X, Wang S, Yang H, Duan X, Dong X (2008) Fabrication and characterization of hexagonal boron nitride powder by spray drying and calcining–nitriding technology Journal of Solid State Chemistry 181:2274-2278 doi:http://dx.doi.org/10.1016/j.jssc.2008.05.029

Shi Z, Huang X, Cai Y, Tang R, Yang D (2009) Size effect of hydroxyapatite nanoparticles on proliferation and apoptosis of osteoblast-like cells Acta Biomaterialia 5:338-345 doi:http://dx.doi.org/10.1016/j.actbio.2008.07.023

Steichen SD, Caldorera-Moore M, Peppas NA (2013) A review of current nanoparticle and targeting moieties for the delivery of cancer therapeutics European Journal of Pharmaceutical Sciences 48:416-427 doi:http://dx.doi.org/10.1016/j.ejps.2012.12.006

Stevenson BR, Begg DA (1994) Concentration-dependent effects of cytochalasin D on tight junctions and actin filaments in MDCK epithelial cells Journal of Cell Science 107:367-375

Tang C, Bando Y, Huang Y, Zhi C, Golberg D (2008) Synthetic routes and formation mechanisms of spherical boron nitride nanoparticles Advanced Functional Materials 18:3653-3661

Trickey WR, Lee GM, Guilak F (2000) Viscoelastic properties of chondrocytes from normal and osteoarthritic human cartilage Journal of Orthopaedic Research 18:891-898

Unciti-Broceta JD, Cano-Cortés V, Altea-Manzano P, Pernagallo S, Díaz-Mochón JJ, Sánchez-Martín RM (2015) Number of Nanoparticles per Cell through a Spectrophotometric Method-A key parameter to Assess Nanoparticle-based Cellular Assays Scientific reports 5

Wood GL, Janik JF, Visi MZ, Schubert DM, Paine RT (2005) New Borate Precursors for Boron Nitride Powder Synthesis Chemistry of Materials 17:1855-1859 doi:10.1021/cm048255p

Wu JCS, Lin Z-A, Pan J-W, Rei M-H (2001) A novel boron nitride supported Pt catalyst for VOC incineration Applied Catalysis A: General 219:117-124 doi:http://dx.doi.org/10.1016/S0926-860X(01)00673-1

Zhang Y, Venugopal JR, El-Turki A, Ramakrishna S, Su B, Lim CT (2008) Electrospun biomimetic nanocomposite nanofibers of hydroxyapatite/chitosan for bone tissue engineering Biomaterials 29:4314-4322 doi:http://dx.doi.org/10.1016/j.biomaterials.2008.07.038

Zhou E, Lim C, Quek S (2005) Finite element simulation of the micropipette aspiration of a living cell undergoing large viscoelastic deformation Mechanics of Advanced Materials and Structures 12:501-512